LA-UR- 01-4441

Approved for public release; distribution is unlimited.

Title:	Local Dynamics of Water on Fused Silica Probed by Individual, Cationic Fluorasent Dye Molecules
Author(s):	William Patrick Ambrose, B-2 Peter M. Goodwin, B-2
Submitted to:	Single Molecules

Los Alamos
NATIONAL LABORATORY

July 31, '01

Local Dynamics of Water on Fused Silica Probed by Individual, Cationic Fluorescent Dye Molecules

W. Patrick Ambrose and Peter M. Goodwin
Los Alamos National Laboratory, Bioscience Division, Los Alamos, NM 87545 USA

Abstract: We investigated the effects of atmospheric humidity on the fluorescence and motion behavior of individual ionic dye molecules on hydrophilic silica. To probe the silica-dye water-condensate system, we observed fluorescence from individual Rhodamine 6G cations ($R6G^+$) on polished amorphous-silica plates (SiO_x) using scanning confocal and polarization-analyzed wide-field total internal reflection microscopies. The $R6G^+$ fluorescence behavior was observed while flowing dry or humidified nitrogen gas over the silica surface. Experiments were performed with a position precision of ~ 100 nm, a time resolution of 6 or 200 ms, and azimuthal angle resolution of a few degrees. Under low or high humidity, individual $R6G^+$ on silica exhibited stochastic intensity fluctuations. At low humidity, translational diffusion of $R6G^+$ was not resolved, however, orientation fluctuation events were observed. Some of the intensity fluctuation events were accompanied by resolvable reorientation. At high humidity, reorientation fluctuations occurred more frequently. Some of the molecules exhibited translational diffusion at high humidity. These studies provide information on the local dynamics of water adsorbed on hydrophilic fused silica under ambient conditions, which we compared to results for water on the crystalline oxide surfaces of mica and MgO. Our conclusion is that water adsorbed at low humidity on silica is immobile, but the additional water adsorbed at high humidity forms diffusing aggregates that can screen the surface siloxanes and solvate $R6G^+$. Motion-intensity fluctuation events are related to brief solvation by diffusing water clusters.

Introduction

A puzzle emerges when comparing results for fluorescence measured from individual dye molecules on glass – sometimes they move, and sometimes they do not. We examined the fluorescence behavior of individual dye molecules and found that atmospheric humidity is an important determinant for the orientation, position, and photostability of soluble ionic dye molecules on the surface of silica in air. This result helps to explain disparate results found in the literature, and solves a potential difficulty for single molecule detection in a humid climate.

Optical detection of individual molecules is performed commonly by diluting molecules of interest in a sea of transparent condensed matter so that they become spatially or spectrally resolvable, exciting molecules using a focused laser beam, and by observing optical transitions by collecting and counting scattered or emitted photons. [Basché 1997] The position, orientation, and photophysical properties of a probe molecule fluctuate with the motions of nearby charges and atoms. It is possible to obtain information on the local behavior of condensed matter by observing the time dependent properties, or trajectories, expressed in single molecule signals. A large variety of condensed matter systems have been probed with single molecules ranging from solid crystals at liquid helium temperatures [Basché 1997] to liquids at room temperature [Ambrose 1999]. In all cases, individual probe molecules are found that exhibit fluctuations in their luminescence properties.

Measurement of the polarized absorption of individual dye molecules on fused silica led to the conclusion that intensity fluctuations occur without resolvable motion [Xie 1994]. Intensity fluctuations are often attributed to fluctuating photophysical properties. Fluctuating photophysical properties at room temperature are impressed on single molecule luminescence signals as spectral shifts [Trautman 1994], changes in decay rates [Ambrose 1998], and changes in intensity accompanying different charge states [Dickson 1997]. In these instances, probe

molecules report on thermally or optically induced internal motions or report on changes in the medium surrounding the molecule. [Xie 1997]

Occasionally, external motion (center of mass or orientation) of dye molecules has been observed. [Ha 1996, 1998, 1999] Also in a different set of papers, Rhodamine 6G cations ($R6G^+$) on silica were found to move, or not move. In one study, the positions of $R6G^+$ on silica were stable within the position accuracy of ~ 100 nm over a period of 8 days. [Ambrose 1994] An upper limit for the diffusion constant for 2-D translation in this example was less than 10^{-8} $\mu m^2/s$. In another study, measurable diffusion of $R6G^+$ on silica clearly was observed on a shorter time scale of hours with a larger diffusion constant of 6.7×10^{-7} $\mu m^2/s$. [Ruiter 1997] So far, no discussion is published to account for the differences in these results. As a tantalizing clue to why the results are different, no motion was observed in desert [Xie 1994] or juniper-conifer transition zones [Ambrose 1994], but motion was resolved in regions close to large bodies of water, i.e., the Pacific Ocean [Ha 1996, 1998, 1999] or the English Channel [Ruiter 1997].

The relative immobility of most dye molecules on silica is surprising in light of a recent prediction from high vacuum studies for the amount of water on hydrophilic silica -- under any terrestrial atmospheric condition there should be more than one third of a monolayer of adsorbed water on hydrophylic silica.[Sneh 1996] Because soluble ionic-dye molecules on silica are usually found to be immobile, single molecule spectroscopists have rarely considered the possible role that atmospheric humidity plays in the dynamics observed in single molecule studies on solid surfaces.

A hint for why water soluble dye molecules are rarely observed to move on silica comes from the results of studies of water adsorbed to other oxide surfaces. The low frequency

dielectric dynamics of water have been studied on a different silicon oxide surface, crystalline mica, using scanning polarization force microscopy.[Xu 1998] From the results of SPFM, one concludes that water on mica forms an immobile first layer at low humidity, but forms mobile aggregates at high humidity. Molecular dynamics simulations for water on MgO have produced similar results, i.e., an immobile first layer and mobile aggregate overlayers.[Marmier 1998]

In this paper, we explicitly tested the hypothesis that atmospheric water adsorbed at high humidity forms mobile aggregates and whether these fluctuating micro droplets produce measurable orientation fluctuations and translational diffusion of $R6G^+$ on hydrophilic silica. There are a variety of proposed and demonstrated methods for determining the transition-dipole orientations of individual molecules [Weiss 1996], [Macklin 1996], [Betzig 1993], [Xie 1998], [Dickson 1998], [Bopp 1998]. A molecule's emission rate varies with angle θ between the transition dipole μ and the optical excitation electric field E as $|\mu \bullet E|^2 \sim \cos^2(\theta)$, which can be used to measure changes in the orientation of the molecule. For measurements of reorientation, we adopted a method that determines the surface azimuth only, since the azimuth is sufficient for obtaining information on orientation fluctuation events. For translational motion, we used far-field imaging techniques to observe changes in position. We found at low relative humidity that the positions were constant and the orientations occasionally fluctuated. Under high humidity, translational diffusion was observed for some molecules and more rapid reorientation was observed for many others. Hence, single molecule measurements can be used to investigate the local properties of small amounts of water adsorbed to the dye-silica system. We conclude that the sub-monolayer of water on silica at low humidity is relatively immobile and does not induce resolvable motion of $R6G^+$. Overlayer aggregates are formed at higher humidity that diffuse

across the surface and produce orientation and position fluctuation events as $R6G^+$ are briefly solvated into the droplets and then readsorbed to the surface.

Experimental Details

Samples consisted of $R6G^+$ adsorbed on nominally dry fused silica. Fused silica (Esco Products) was cleaned by sonicating in soap (Micro 8790-00, Cole Parmer, a mixture of ionic and non-ionic surfactants), ultra pure water (Milli-Q) and methanol, rinsing with water, soaking in sulfuric acid for a few minutes, and alternately rinsing and ultra-sounding many times in water and methanol. After washing, a visible film of water was removed mechanically with flowing nitrogen gas. The properties of the surface of silica depend on chemical treatment and ambient environment. The surface of silica that is cooled from several hundred degrees centigrade consists of bridge bonded oxygens (Si-O-Si), which tend to be hydrophobic. When treated with strong acids or bases, the bridge bonds break and the surface acquires weakly acidic hydrophilic silanols (Si-O-H). In our preparation procedure, the acid wash step produced a hydrophilic surface, as qualitatively determined by observing the decreased surface-water contact angle and increased wettability. Rhodamine 6G perchlorate was dissolved and diluted in methanol to concentrations of $3x10^{-10}$ M or 10^{-8} M for preparation of low and higher coverage surfaces. Rhodamine 6G was deposited by spin coating the methanol solutions on silica samples while allowing the R6G/methanol to evaporate in air.

Images were obtained under ambient air, flowing dry nitrogen gas, or humidified nitrogen gas. Humidified nitrogen gas was produced by bubbling dry nitrogen gas through a 7 cm depth of water at a gas flow rate of ~ 1 mL/sec in a 100 mL flask. The temperatures of the sample, gas and water were equilibrated at a value of ~ 21 C. The quantity of water accumulated on the

silica surfaces under flowing humidified nitrogen was never large enough to produce visible light scatter (no fogging or droplets visible to the human eye).

Fluorescence from individual $R6G^+$ molecules on silica surfaces was observed using fluorescence imaging microscopies. Confocal laser scanning microscopy (CLSM) was used to produce excitation images of the locations and intensities of individual molecules. CLSM was performed by scanning the surface of a silica disk across a focused laser beam (approximately 0.4 μm diameter focused spot) with a piezoelectric-tube positioner. For CLSM, spectrally-filtered fluorescence was detected with a photon counting silicon avalanche photodiode (EG&G). Wide-field microscopy was used to obtain polarization-analyzed emission images. Wide field microscopy was performed by exciting the molecules with through-objective total internal reflection (TIR) microscopy with an illumination region approximately 10 μm in diameter [Ambrose Cytometry paper]. Emission from many individual molecules was imaged onto an intensified CCD camera (Pentamax, intensified and cooled full-frame transfer charge coupled device camera, Princeton Instruments). For emission polarization measurements, the fluorescence images were split using a polarization-analyzing calcite beam displacer. For either confocal or wide-field microscopies, excitation light from an Argon ion laser operating at 514.5 nm wavelength was delivered to a sample and fluorescence was collected through a high numerical aperture microscope objective (Zeiss 100x 1.3 NA Fluar for confocal and Zeiss 63X 1.4 NA Planapo for wide-field). The excitation power at the sample was in the microwatt range for CLSM and in the milliwatt range for widefield microscopy, well below optical saturation in either case [Ambrose 1997].

Polarization-analyzed wide-field movies obtained with TIR excitation were setup and analyzed with the following approximations. Previous angle-analyzed absorption and emission

measurements revealed that ensembles of $R6G^+$ lay flat on silica with emission dipoles distributed within 16 degrees of the surface plane [Huston 1989, Lieberherrer 1987]. Under dry conditions, $R6G^+$ mostly probes the in-plane components of the excitation field. To reduce the polarization bias effect of the excitation field, the two components of the TIR excitation evanescent field in the surface plane were adjusted to have approximately circular polarization. This was accomplished by using a higher coverage of $R6G^+$ on silica under dry conditions. A lower excitation power was used for lower rates of photobleaching during the setup procedure. The input polarization was adjusted with quarter wave and half wave plates and the calcite analyzer was rotated while balancing the intensity in the conjugate images. The net effect of this procedure was to produce circularly polarized evanescent field components in the surface plane and an unknown component perpendicular to the plane. An absorption dipole with an arbitrary orientation should have excitation contributions from both the circularly polarized in–plane component and the normal component, with an excitation rate that is axially symmetric about the surface normal.

Neglecting for the moment the known polarization mixing effects in high numerical aperture optics [Axelrod 1989, Ha 1999], we used two orthogonal components of each molecule's emission as an approximate measure of orientation fluctuation events. From each molecule, a number of detected photons were measured in two orthogonal polarizations, which we denoted as the intensities $I_{//}$ and $I_{\perp}$ (parallel and perpendicular to an axis in the calcite analyzer). Both of these intensities are proportional to the rate of excitation (symmetric about the surface normal), and are proportional to factors relating the square of the Cartesian components of the field to polar coordinates of the emitting dipole, $(\sin\theta\cos\varphi)^2$ and $(\sin\theta\sin\varphi)^2$, where θ is the angle of the emission dipole with respect to the surface normal and

φ is the angle of its in-plane component with respect to the parallel axis defined by the calcite analyzer. We computed the in-plane (azimuthal) component of the dipole orientation of each of the molecules from $\varphi = \arctan\left(\sqrt{I_\perp / I_{//}}\right)$, where the intensities, $I_{//}$ and $I_\perp$, were obtained from background subtracted signals summed over pixels belonging to a single pair of spots from one molecule. The effects of the out-of-plane excitation and emission components cancel in the ratio $I_\perp / I_{//}$. Without modulating the excitation field, the sign of the azimuth is not obtained [Wiess] and values of φ are reflected into the range 0 to 90 degrees.

The level of systematic error imposed by these approximations was assessed. There are various sources of effective depolarization of the emission. For an emission dipole of arbitrary orientation, a high numerical aperture objective will reform an emission image with components that are a mixture of the emission-field components [Axelrod 1989, Ha 1999]. In the absence of this depolarization effect, the distribution of φ values for $R6G^+$ on a dry surface is expected to be distributed uniformly from 0 to 90 degrees. The systematic error contributions from depolarization during imaging, and the effects of sifting molecules out of images using a threshold above a noisy background produced a systematic distortion of the φ distribution away from 0 and 90 degrees by about 15 degrees. We regard the calculated parameter, $\varphi = \arctan\left(\sqrt{I_\perp / I_{//}}\right)$, obtained from these fluorescence measurements not as a precise value of the azimuth, but as a useful measure for determining the timing and approximate rates of orientation fluctuation events.

To assess whether changes in orientation were resolved, error estimates for φ were calculated from error estimates for the intensified CCD camera measurements. Images of a constant white light field filtered through the single molecule apparatus were recorded with different light levels at the camera plane. The standard deviation and mean in the measured

signal sizes were recorded and used as a look-up table to estimate the expected error in subsequent single intensity measurements.

Results

Figure 1 shows long term fluctuations in fluorescence intensity of individual $R6G^+$ on silica in ambient air with an atmospheric humidity typical in our laboratory, i.e., under conditions we regard as nominally dry (~18 % humidity). The images show repeated traces of fluorescence intensity excited along a single line and stacked along the time axis in the figure. Confocal line scans show the behavior of a few individual molecules repeatedly sampled in short intervals of time (0.1 second sampling intervals taken twice in each 3 second round trip) over a long period of time (600 seconds). In preparation for each experiment, hysteresis drift in the sample scanner was allowed to decay away by repeating the line scan for several minutes before beginning laser illumination and data collection. The straight lines are from molecules that do not diffuse (do not move more than 100 nm in a time interval of ten minutes) and have relatively constant emission intensity. There are other molecules that fluctuate in intensity, sometimes with very dim periods lasting many minutes. The positions of the fluctuating molecules appear to be constant under dry conditions. To test the affect that adsorbed water has on these fluctuations, the remainder of the experiments in this paper were performed under dry or humidified nitrogen gas instead of ambient air.

The fluorescence fluctuations of individual molecules observed with scanning confocal microscopy changed with humidity. The first three panels of Fig. 2 show $R6G^+$ molecules imaged with CLSM under flowing dry N_2. The last three panels show the same region of the sample under flowing, humidified N_2 gas. Under dry conditions (panels A, B, and C), the round

image spots, which are a representation of the laser intensity as viewed by the much smaller molecule, are modulated with dark lines due to intensity fluctuations such as those in Fig. 1. Under humid conditions (panels D, E, and F), the fluctuations are more rapid and the spots are less well defined. The photostability appears to be lower, as well, during exposure to humidified N_2. We have obtained images under dry conditions before and after exposure to humid N_2. In these experiments, the positions of stationary molecules were randomized. We interpret some of the streaky appearance in Fig. 2 as arising from molecules that diffused translationally on the surface exposed to humidified nitrogen.

Next, information was obtained about orientation fluctuation events by analyzing the emission polarization. To observe the orientations of the in-plane components of many individual emission dipoles, we used wide field microscopy with through objective TIR. To analyze the polarizations, the illuminated region was imaged through a calcite polarizing beam displacer. As shown in Fig. 3, the emission image corresponding to the single, 10 μm wide excitation region was split and detected in separate orthogonally-polarized zones in a single camera frame. Each molecule contributed intensity to a pair of spots, one spot in the perpendicular-component image and the other in the parallel-component image. The intensities in the pairs of spots are not equal because under dry flowing N_2 individual $R6G^+$ are relatively static during 0.2 seconds, have polarized emission and have random in-plane orientations.

To observe the time dependence of the azimuthal angle $\varphi(t)$, we obtained repeated images (movies) with an image cycle time of 200 ms. Fig. 4 shows examples of movies of pairs of conjugate spots analyzed into orthogonal polarizations. The orientation behavior of a molecule under dry nitrogen is shown in Fig. 4 (A). In the first 5 image pairs of Fig. 4 (A) (read from left to right), the intensity in the perpendicular channel was strong and the parallel intensity

was weak, i.e., the molecule's dipole azimuth was oriented 75 degrees from the // axis. During the 6th through the 12th images in Fig. 4 (A), the molecule's orientation and conjugate intensities fluctuated. Subsequent to this orientational wandering over a period of 1.4 seconds, the orientation became stable again, but at a new angle of 15 degrees. Under dry nitrogen, the positions of $R6G^+$ molecules did not change measurably, but occasionally they underwent large orientation fluctuations.

As observed with scanning confocal microscopy, different types of behavior became more prevalent in wide-field TIR movies when the humidity was increased. Fig. 4 (B) shows examples of conjugate pairs of spots from several molecules in the same region. There is a bright spot from a molecule (labeled 1) that did not reorient or translate. Another set of molecules such as those labeled 2, 3 and 4 diffused translationally. The diffusing molecules often had nearly equal intensities in the two emission polarizations.

Many examples of $\varphi(t)$ extracted from movies such as those in Fig. 4 are shown in Fig. 5. Each panel shows data from a different molecule. The upper set of panels in Fig. 5 (1)-(18) were obtained under dry nitrogen, and the lower set of panels (19)-(36) were obtained under humidified nitrogen. Hundreds of molecules were observed in two dry movies and four humid movies. The subsets of molecules shown in Fig. 5 were selected on the basis of lowest relative error in the angle diffusion coefficients (described in more detail below). Angle error bars in the figures were computed from intensity error estimates, which were obtained from a separate analysis of the intensified-camera intensity noise at different light levels. When one of the conjugate spot intensities for a molecule lay near zero, background noise fluctuations and background subtraction sometimes resulted in negative signals. For negative intensity ratios in the square root, the angle was set to the closest appropriate limiting value of 0 or 90 degrees.

Missing angle points in Fig. 5 correspond to dim periods in both conjugate spots. It was noted in trial runs that under humid conditions the molecules bleached more readily; the humid movies were recorded for a shorter time period than the dry movies.

Many types of behavior were observed for $\varphi(t)$ in the dry movies. For some molecules, the azimuthal orientation changed slowly or not at all (Fig. 5 (1)-(7)). Other molecules exhibited a resolvable shift in orientation after a long dark period (Fig. 5 (8) and (9)). Still others had dark periods without a measurable reorientation (angle shift smaller than the angle error estimates (Fig. 5 (1), (12), (16))). In the dry cases, there are also molecules that seem to toggle between a subset of angles with abrupt orientation fluctuation jumps (Fig. 5 (10) and (11)), or wander around but without completely averaging to equal conjugate intensities on the 0.2 second integration time period (Fig. 5 (12)-(18)). In the humid cases, occasionally molecules were found with stable positions and orientations (as in Fig. 4 (B)). However, as in Fig. 5 (19)-(36), it was much more common to observe a more rapid or diffusive variation in the angle under humid conditions.

For statistical comparison of the orientation behavior under dry and humid conditions, we chose as an approximate measure of the rate of azimuthal reorientation an angle diffusion coefficient computed from the $\varphi(t)$ data. The angle diffusion coefficient, D_φ, was obtained by fitting the mean square variation in $\varphi(t)$, i.e., $<(\varphi(t)-\varphi(0))^2>$, by a straight line, $4D_\varphi t + D_0$, where D_0 was included to account for random fluctuations arising from intensity noise. An error estimate dD_φ was obtained also by propagating intensity error estimates through the calculation of $\varphi(t)$ and $<(\varphi(t)-\varphi(0))^2>$. In the analysis of molecules from the polarization-analyzed movies, there were sources of artifacts that produced redundancy in the $\varphi(t)$ traces. A simple procedure was included to track molecules that translationally diffused, such as those in Fig. 4.

Occasionally, a pair of molecules would become unresolved spatially. Molecules with redundancies were thrown out of the final distributions. To be able to compare the results for the dry and humid movies, D_φ and N were computed for the first 30 frames (6 seconds) for both the dry and humid movies.

Figure 6 is a scatter plot of the individual D_φ results plotted against the corresponding total number of detected photons, N. Each point is from a single molecule. Humid and dry conditions are distinguished by circles and squares, respectively, and plotted against linear axes. The same data are shown on logarithmic axes in the inset. The stochastic nature of photobleaching, intensity fluctuations, and the heterogeneous nature of the molecular environments produced a wide variability in the joint distribution of D_φ and N. A wide variation in the intensity error estimates also led to a wide distribution of dD_φ error estimates. To indicate the relative confidence of values in Fig. 6, molecules were grouped by relative error in D_φ, i.e., by dD_φ / D_φ. Instead of indicating the absolute error estimate in the scatter plot, the size of the points in Fig. 6 are related to the level of confidence, i.e., large points have the highest confidence in D_φ (the largest points have the lowest relative error dD_φ / D_φ). Refer to the figure caption for numerical details. The scatter plot in Fig. 6 reveals correlated changes in two of the fluorescence parameters. Under dry conditions, $R6G^+$ typically were more orientationally stable (had lower D_φ) with larger numbers of photons detected in a 6 sec time period. When the humidity was increased, more rapid orientation fluctuations were observed and the number of detected photons was reduced.

Discussion

Under low or high humidity, the range of behaviors of individual molecules on silica was very heterogeneous. Despite this heterogeneity, the absence or presence of water in the gas phase above the sample produced clear changes in the distributions. Under low humidity, typical $R6G^+$ cations exhibited fluctuations in intensity and orientation, with a mean time between the largest orientation fluctuation events of 4 seconds, and typically did not translate more than 100 nm in several days.

At high humidity, translational and orientational diffusion were much more rapid. As seen in the wide field images with 200 ms integration times, apparent speeds for some of the fluorescent spots were several hundred nm per second (Fig. 4 (B)). In the confocal scanning images, these diffusing molecules appeared as streaks (Fig. 2 (D)) since despite the higher pixel rate of 6 ms / pixel, the scan round trip time of several seconds was slower than the wide-field image integration time of 200 ms. Translational motion for other molecules was not resolved, but the angles jumped often enough on the 0.2 second time scale to produce a diffusive $\varphi(t)$ in many of the apparently stationary molecules.

Despite the prediction that hydrophilic silica has at least a third of a monolayer of water under any normal combination of terrestrial humidity, temperature, and pressure,[Sneh] dye molecules at the silica-air interface have very stable positions at modest humidity. The reason dye molecules on silica are not continuously moving may be because the mobility and solvation capacity of the first layer of water is low. On oxide surfaces, dielectric measurements indicate that the movement of water is restricted. Liquid water has a dielectric polarization-relaxation peak near 2.5 GHz. Mixtures of silica particles in water exhibit a dielectric loss peak at a much

lower frequency of 1 MHz [Ishida 1999], which is interpreted as a restricted water-dipole reorientation rate at the surface of the silica.

On a different silicate surface, namely mica, water adsorbed from air exhibits a humidity dependent dielectric response when observed with scanning polarization force microscopy (SPFM) [Xu 1998]. The roll-off frequency in the dielectric response as measured by SPFM varies from low values of 27 kHz at high humidity down to very low values of approximately 1 Hz at low humidity. SPFM reveals that below 20 % humidity at room temperature water adsorbed on mica is relatively immobile. At humidities higher than 20% at room temperature, the SPFM results indicate that mobile islands of liquid water condense on top of the immobile layer on mica.

Molecular dynamics simulations on a different oxide surface, MgO, exhibit a behavior similar to the experimental results on mica. The first layer of water molecules is relatively stable at room temperature and overlayers tend to aggregate into islands [Marmier 1998]. Likewise, UHV measurements of water on silica with 100% silanols revealed that the water-silica desorption energy was lower than the water-water condensation energy. One anticipates that at coverages of approximately one monolayer of water on silica, island overlayer formation may begin before completion of a continuous first immobile layer [Sneh 1996].

It is not immediately clear that water on amorphous silica with silanols should behave as the water on crystaline mica and MgO. The coverage and nature of water on amorphous silica probably depends also on the percent composition of bridge-bonded oxygens and silanols and the local surface structure. The local surface structure is not completely flat. Fractal analysis and extrapolation of the local surface tilt angles measured in atomic force microscopy (AFM) down to molecular dimensions yields a distribution of surface tilts peaked near 15 degrees [Simpson

1999]. The distribution of Rhodamine 6G dipoles on silica was found to lay within 16 degrees of the surface plane [Huston 1991, Lieberherr 1987] which is consistent with the AFM extrapolation if the rings of $R6G^+$ attempt to lay flat on the silica (presumably all of these results were obtained under low humidity).

Figure 7 summarizes our view of the environment of dye molecules on hydrophilic silica as determined from the behavior of individual $R6G^+$ and by comparison to ensemble measurements on other oxide-surface systems. It was suggested that the weakly acidic silanols will donate protons to water and produce charge separation dipoles oriented normal to the surface ($SiO^-...H_3O^+$) [Sneh 1996]. Cationic $R6G^+$ on silica under ambient conditions probably associates coulombically with $SiO^-...R6G^+$. Under low humidity, $R6G^+$s may associate also with a few water molecules in the first immobile layer. At low humidity, the amount of water is small enough that $R6G^+$s are not fully hydrated and rarely dissociate from the silica. As the humidity increases, the immobile layer increases in coverage and mobile water begins to accumulate. Since stable molecules are observed under high humidity, the coverage of mobile water is not complete, i.e., the mobile water aggregates into islands. Since we do observe translational motion for some of the molecules, this suggests that the liquid islands are not static, but perhaps similarly to mica and MgO diffuse on the immobile layer. As the liquid islands diffuse over the bound $SiO^-...R6G^+$, the $R6G^+$ molecules may alternately dissolve into the liquid and rebind by displacing other $SiO^-...H_3O^+$. As the size and number of liquid islands increases with higher humidity, the frequencies of solvation and rebinding, and the rates of orientational and translational fluctuation events should increase. Additionally, the water clusters may be in dynamic equilibrium with atmospheric water and fluctuate in and out of existence.

We caution that hydration fluctuations are probably not the only source of intensity fluctuations; hydration fluctuations contribute to the overall sources of fluctuation. Fluctuations of photophysical properties have been observed for hydrophobic DiICx on flame treated silica (hydrophobic Si-O-Si, with decreased Si-O-H coverage). These fluctuations apparently do not change with increased humidity [Weston 1999]. Photophysical fluctuations and position changes are also noted for molecules in a thin non-ionic polymer layer on silica.[Meixner? New Weston Paper? Science paper?] These fluctuations probably are not water mediated, but could reflect changes in the local structure of the polymer or other type of polar but non-ionic over layer from the ambient atmosphere. Since the intensity fluctuations for $R6G^+$ on silica sometimes are observed to correspond with reorientation, and sometimes not, we conclude that at least one source of fluctuation is from water mediated orientation, but there must be other sources, as well.

In summary, we have demonstrated that single molecule detection using a cationic dye molecule on hydrophilic fused silica can provide information on the behavior of adsorbed water. In particular, a fraction of a monolayer of water predicted at low humidity appears to be immobile and unable to fully solvate $R6G^+$ dye molecules. At higher humidity, fluctuating islands of water are formed that are able to solvate the ionic dye $R6G^+$ and diffuse on top of the immobile water silica surface.

References

W. P. Ambrose, P. M. Goodwin, J. C. Martin, and R. A. Keller, Science **265**, 364-367 (1994).

W. Patrick Ambrose, Peter M. Goodwin, Jörg Enderlein, David J. Semin, and Richard A. Keller, Proc. of the Society of Photonics and Instrumentation Engineers (SPIE), **3270** (Methods for Ultrasensitive Detection), 190-199 (1998).

W. P. Ambrose, P. M. Goodwin, J. H. Jett, A. Van Orden, J. H. Werner, and R. A. Keller, Chemical Reviews. Thematic Issue: Chemical Analysis in Small Domains **99**, 2929-2956 (1999).

W.P. Ambrose, P.M. Goodwin, and J.P. Nolan, Cytometry **36**, 224-231 (1999).

W.P. Ambrose, P.M. Goodwin, J. Enderlein, D.J. Semin, J.C. Martin, and R.A. Keller, Chem. Phys. Lett. **269**, 365-370 (1997).

Axelrod depolarization with NA paper.

Single-Molecule Optical Detection, Imaging and Spectroscopy, Eds. T. Basché, W. E. Moerner, M. Orrit, and U. P. Wild, (VCH Verlagsgesellschaft mbH, Weinheim, 1997).

E. Betzig and R.J. Chichester, Science 262, 1422-1425 (1993).

M.A. Bopp, A.J. Meixner, G. Tarrach, I. Zschokke-Gränacher, L. Novotny, Chem. Phys. Lett. **263**, 721-726 (1996).

M.A. Bopp, Y.J. Haran, E.A. Morlino, and R.M. Hochstrasser, Appl. Phys. Lett. **73**, 7-9 (1998).

R.M. Dickson, A.B. Cubitt, R.Y. Tsien, and W.E. Moerner, Nature **388**, 355-358 (1997).

R.M. Dickson, D.J. Norris, and W.E. Moerner, Phys. Rev. Lett. **81**, 5322-5325 (1998).

F. Güttler, M. Croci, A. Renn, and U.P. Wild, Chem. Phys. **211**, 421-430 (1996).

T. Ha, Th. Enderle, D.S. Chemla, P.R. Selvin, and S. Weiss, Phys. Rev. Lett. **77**, 3979-3982 (1996).

T. Ha, J. Glass, Th. Enderle, D.S. Chemla, and S. Weiss, Phys. Rev. Lett. **80**, 2093-2096 (1998).

T. Ha, T.A. Laurence, D.S. Chemla, and S. Weiss, J. Phys. Chem. B **103**, 6839-6850 (1999).

G.S. Harms, M. Sonnleitner, G.J. Schütz, H.J. Gruber, and Th. Schmidt, Biophysical Journal 77, 2864-2870 (1999).

A.L. Huston and C.T. Reimann, Chem. Phys. **149**, 401-407 (1991).

T. Ishida and T. Makino, J. Coll. Interf. Sci. **212**, 144-151 (1999).

M. Lieberherr, C. Fattinger, and W. Lukosz, Surf. Sci. **189**, 954-959 (1987).

A.Marmier, P.N.M. Hoang, S. Picaud, C. Girardet, R.M. Lynden-Bell, J. Chem. Phys. **109**, 3245-3254 (1998).

J.J. Macklin, J.K. Trautman, T.D. Harris, and L.E. Brus, Science **272**, 255-258 (1996).

R. Rigler, Ü. Mets, J. Widengren, and P. Kask, European Biophysical Journal **22**, 169-175 (1993).

A.G.T. Ruiter, J.A. Veerman, M.F. Garcia-Parajo, and N.F. van Hulst, J.Phys. Chem. A **101**, 7318-7323 (1997).

I.Sase, H. Miyata, S. Ishiwata, and K. Kinosita, Jr., Proc. Natl. Acad. Sci. USA **94**, 5646-5650 (1997).

Th. Schmidt, G.J. Schutz, W. Baumgartner, H.J. Gruber, and H. Schindler, Proc. Natl. Acad. Sci. **93**, 2926-2929 (1996).

J. Sepiol, J. Jasny, J. Keller, U.P. Wild, Chem. Phys. Lett. **273**, 444-448 (1997).

G.J. Simpson and K.L. Rowlen, J. Phys. Chem. B **103,** 1525-1531 (1999).

G.J. Simpson and K.L. Rowlen, J. Phys. Chem. **103,** 3800-3811 (1999).

O.Sneh, M.A. Cameron, and S.M. George, Surf. Sci. 364, 61-78 (1996).

C. Tietz, R. Daum, A. Dräbenstedt, J. Schuster, L. Fleury, A. Gruber, J. Wrachtrup, C. von Borczyskowski, Chem. Phys. Lett. **282,** 164-170 (1998).

J.K. Trautman, J.J. Macklin, L.E. Brus, and E. Betzig, Nature 369, 40-42 (1994).

K.D. Weston and S.K. Buratto, J. Phys Chem. A **102,** 3635-3638 (1998).

K.D. Weston, P.J. Carson, H. Metiu, and S.K. Buratto, J. Chem. Phys. **109,** 7474-7485 (1998).

X.S. Xie and R.C. Dunn, Science **265,** 361-364 (1994).

H.P. Lu and X.S. Xie, Nature **385,** 143-146 (1997).

X.S. Xie and J.K. Trautman, Annu. Rev. Phys. Chem. **49,** 441-480 (1998).

L. Xu, A. Lio, J. Hu, D. F. Ogletree, and M. Salmeron, J. Phys. Chem. B **102,** 540-548 (1998).

Figure Captions

Figure 1. Long time-scale intensity fluctuations of individual Rhodamine 6G molecules on silica. These images were obtained under ambient air near 20 C with approximately 18 % relative humidity (the outdoor humidity was 43% at 10 C, which we calculated to be 18% within our lab at 20 C). Fluorescence emission photons were detected and counted while a silica sample was scanned repeatedly on the same line. The upper and lower panels show different line-scan images at arbitrarily chosen positions. The intensity data collected in one direction of a 15 micrometer scan were binned in 200 pixels and repeated 200 times with 3 seconds per round trip over a period of 10 minutes. Since the signals cover a wide dynamic range, the logarithm of the data was taken and displayed on a linear gray scale. The laser power at the sample was 1.2 microwatts and the most intense (white) signals were ~$5x10^4$ counts/sec.

Figure 2. Fluorescence images obtained under flowing dry and humidified nitrogen gas. Confocal laser scanning fluorescence images of individual Rhodamine 6G molecules on silica were repeated in the same region of the sample while flowing dry nitrogen (panels (A), (B), and (C))and then flowing humidified nitrogen over the sample (panels (D), (E), and (F)). Addition of water vapor to the flowing nitrogen gas resulted in more rapid intensity fluctuations and increased rates of photobleaching. The horizontal, fast-scanning axis round-trip time was 2.4 seconds. Each image shows fluorescence acquired in one scan direction in 200x200 pixels at 6 *ms / pixel for a total image time of 8 minutes. The panels shown in the figure are* 7x7 μm^2 subsets of raw images acquired in an area of 15x20 μm^2. The emission data are displayed with a linear gray scale that ranges from 100 kcps to 134 kcps for a laser power of 2.6 microwatts at

514.5 nm excitation wavelength. An upward drift in the scanner position is apparent in (A), (B), and (C). For lack of reference points in (D), (E), and (F), the customary practice of drift removal was not performed.

Figure 3. Conjugate emission-polarization analyzed images of single molecules of $R6G^+$ under flowing dry nitrogen. $R6G^+$ on silica was excited with through objective TIR using ~ 1 mW of 514.5 nm wavelength laser light in a region 10 μm in diameter. The components of the evanescent field in the silica surface were approximately circularly polarized. Emission images were split with polarization analyzed parallel or perpendicular to the horizontal direction in the figure. The image pairs were displaced effectively 16.7 microns and projected onto an ICCD. The scale bar on the lower left is 10 μm. This image was obtained with an integration time of 0.2 seconds, and the total signal (sans background) integrated over the brighter spots was about 2000 detected photons.

Figure 4. Example time series of conjugate-polarization images for individual $R6G^+$ molecules on silica under flowing dry and humidified nitrogen gas. The analyzed emission polarizations are indicated on the left. The molecule in (A) was imaged under dry nitrogen, and exhibited both stable and fluctuating orientation without translation. Under humidified nitrogen, (B), both stable and diffusing molecules were observed. Note the similar intensities in the two spots for diffusing molecules labeled 2 through 4. The data were displayed on a linear gray scale after subtracting the background and taking the square root of the intensity.

Figure 5. Azimuthal angle fluctuations under dry and humid conditions. Examples are displayed for the time varying azimuthal angle $\varphi(t)$ of the emission dipole moment projection into the surface for individual $R6G^+$ molecules. Panels (1)-(18) were obtained under dry N_2, and panels (19)-(36) were obtained under humidified N_2. These examples are from movies such as Fig. 4 obtained with 0.2 second image integration times.

Figure 6. Scatter plots of the angle diffusion coefficient D_φ versus the total number of detected photons from individual $R6G^+$ on silica. Squares were obtained under dry conditions. Circles were obtained under humidified conditions. The sizes of the points represent confidence levels in D_φ. The largest points have the lowest relative error dD_φ / D_φ. The relative error ranges for various groups of points from the largest to smallest points are dD_φ / D_φ = (0.0 to 0.4), (0.4 to 0.8), (0.8 to 2.0), (2.0 to 4.0), and (4.0 to 8.0). Despite a wide variability in values, there is a clear trend towards more frequent motion events and photochemical instability at high humidity.

Figure 7. Model for the behavior of water and ionic dye molecules on silica in air. At low humidity in air (A), there is always some water on silica, but these surface-bound water and dye molecules are immobile. At high humidity, (B)-(D), water overlayers aggregate into diffusing clusters. Occasionally, a water cluster collides with a $R6G^+$ as depicted in (C), resulting in brief solvation, orientation, and translation fluctuation events.

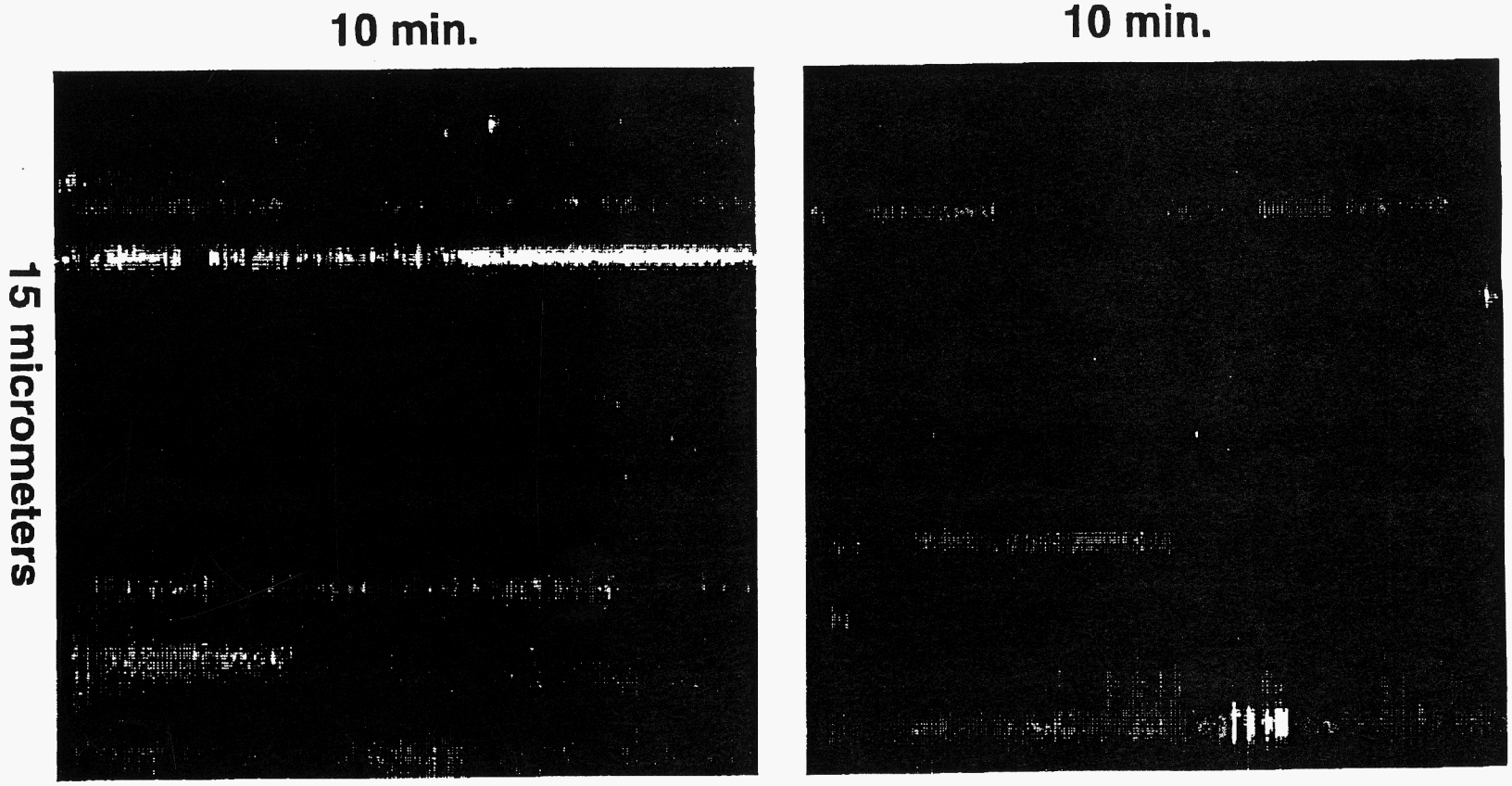

Fig. 1

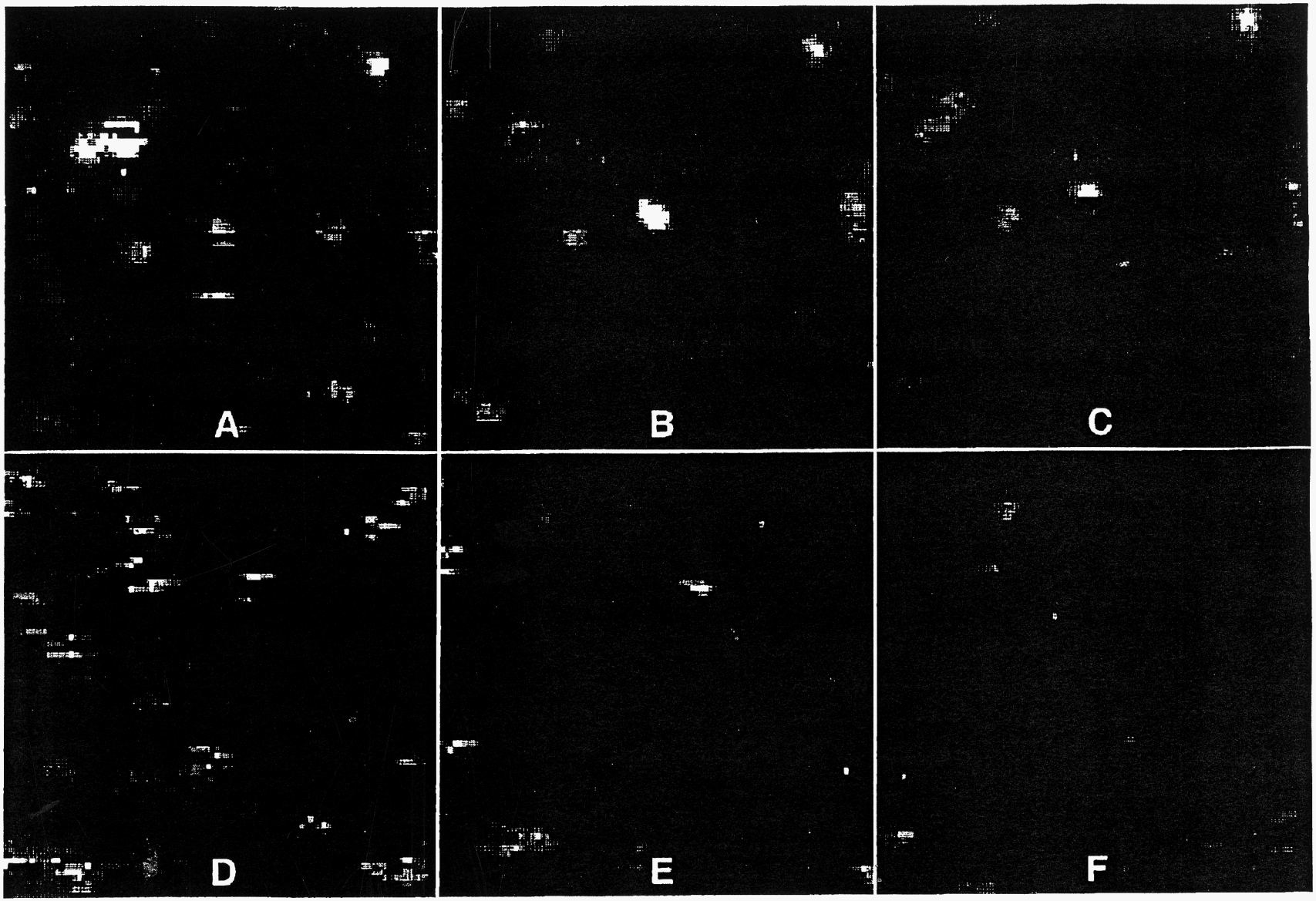
A
B
C
D
E
F

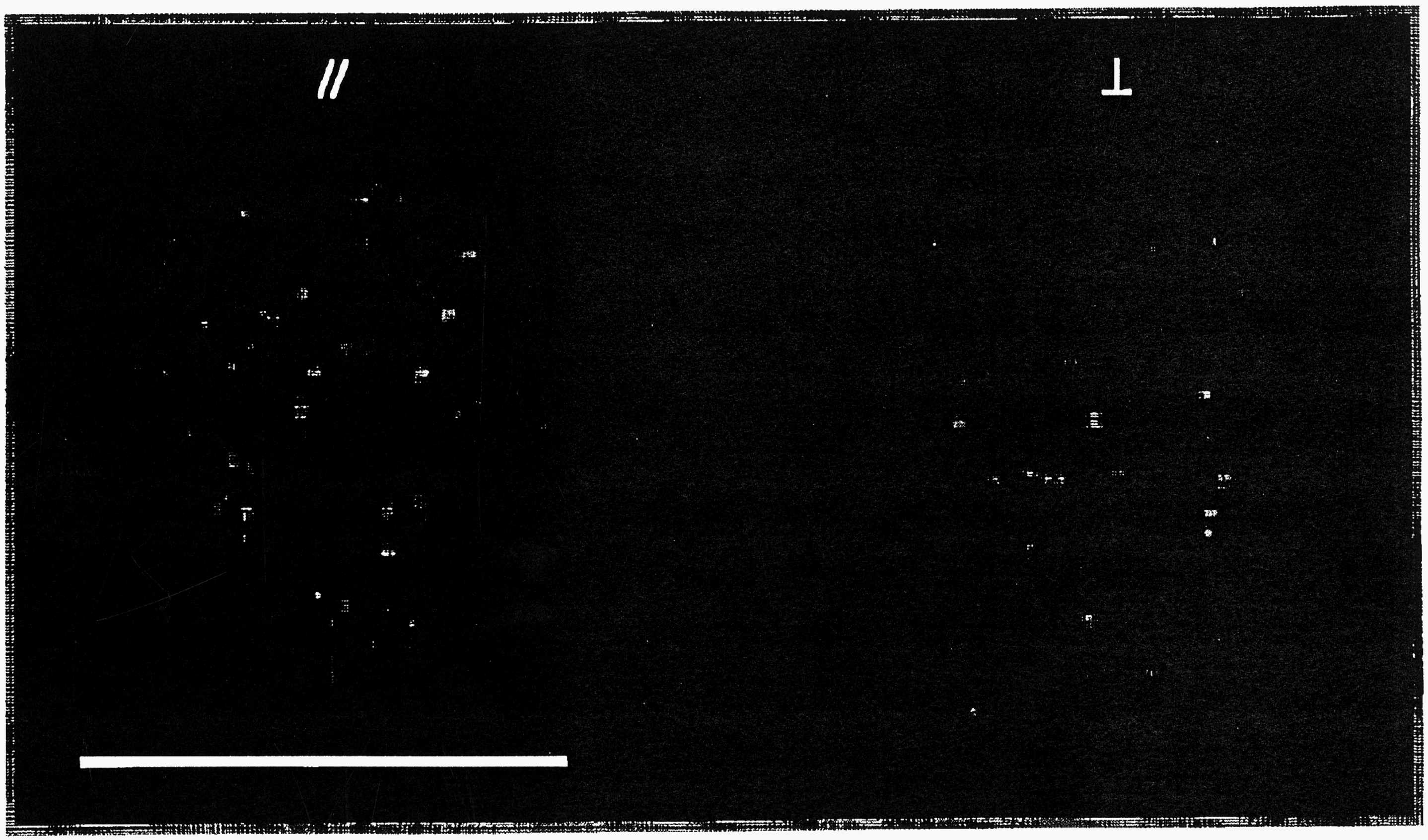

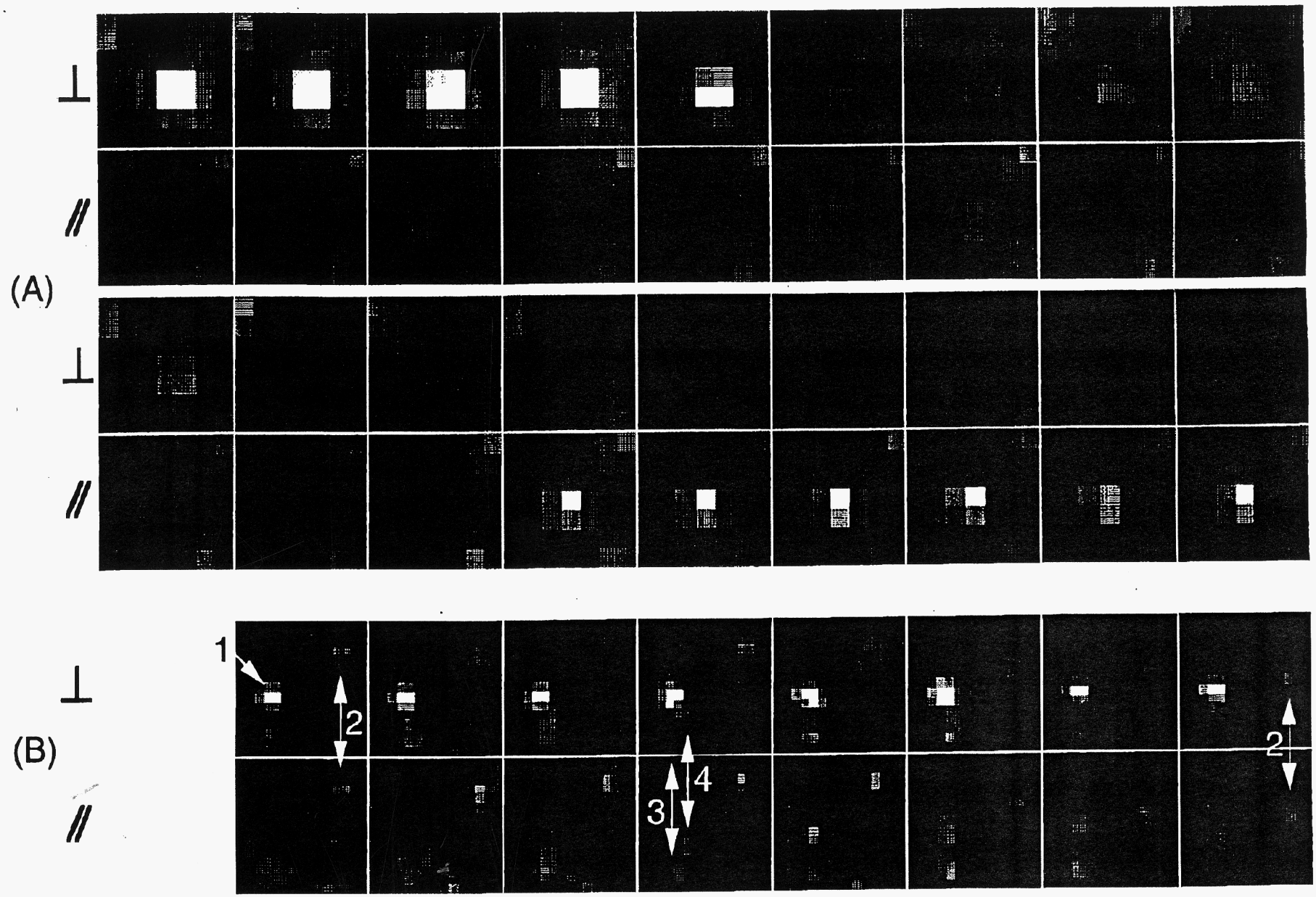
(A)
⊥
//
⊥
//
(B)
⊥
//
1
2
3
4
2

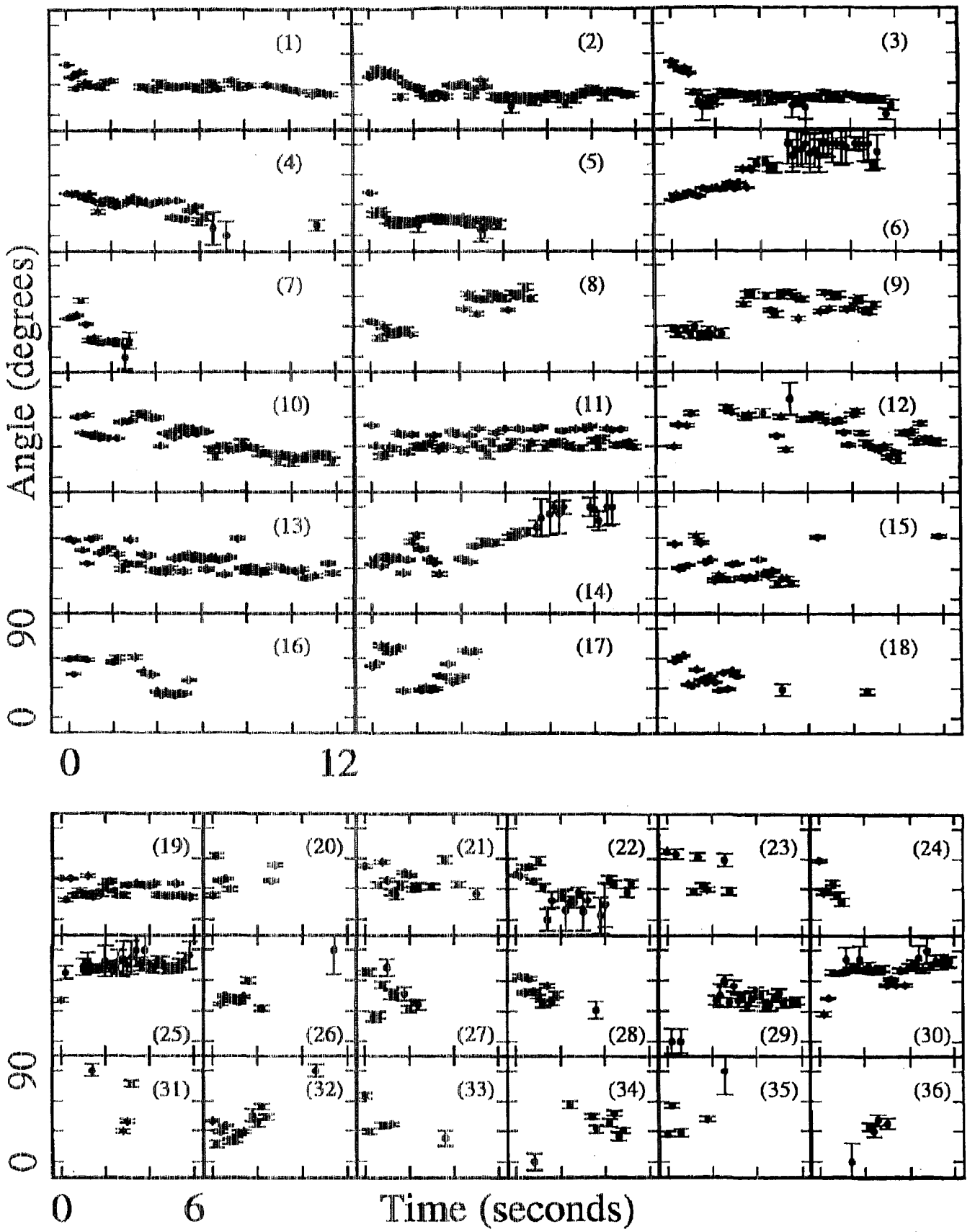
(1)
(2)
(3)
(4)
(5)
(6)
(7)
(8)
(9)
(10)
(11)
(12)
(13)
(14)
(15)
(16)
(17)
(18)
Angle (degrees)
0
90
0
12
(19)
(20)
(21)
(22)
(23)
(24)
(25)
(26)
(27)
(28)
(29)
(30)
(31)
(32)
(33)
(34)
(35)
(36)
0
90
0
6
Time (seconds)

Fig. 5

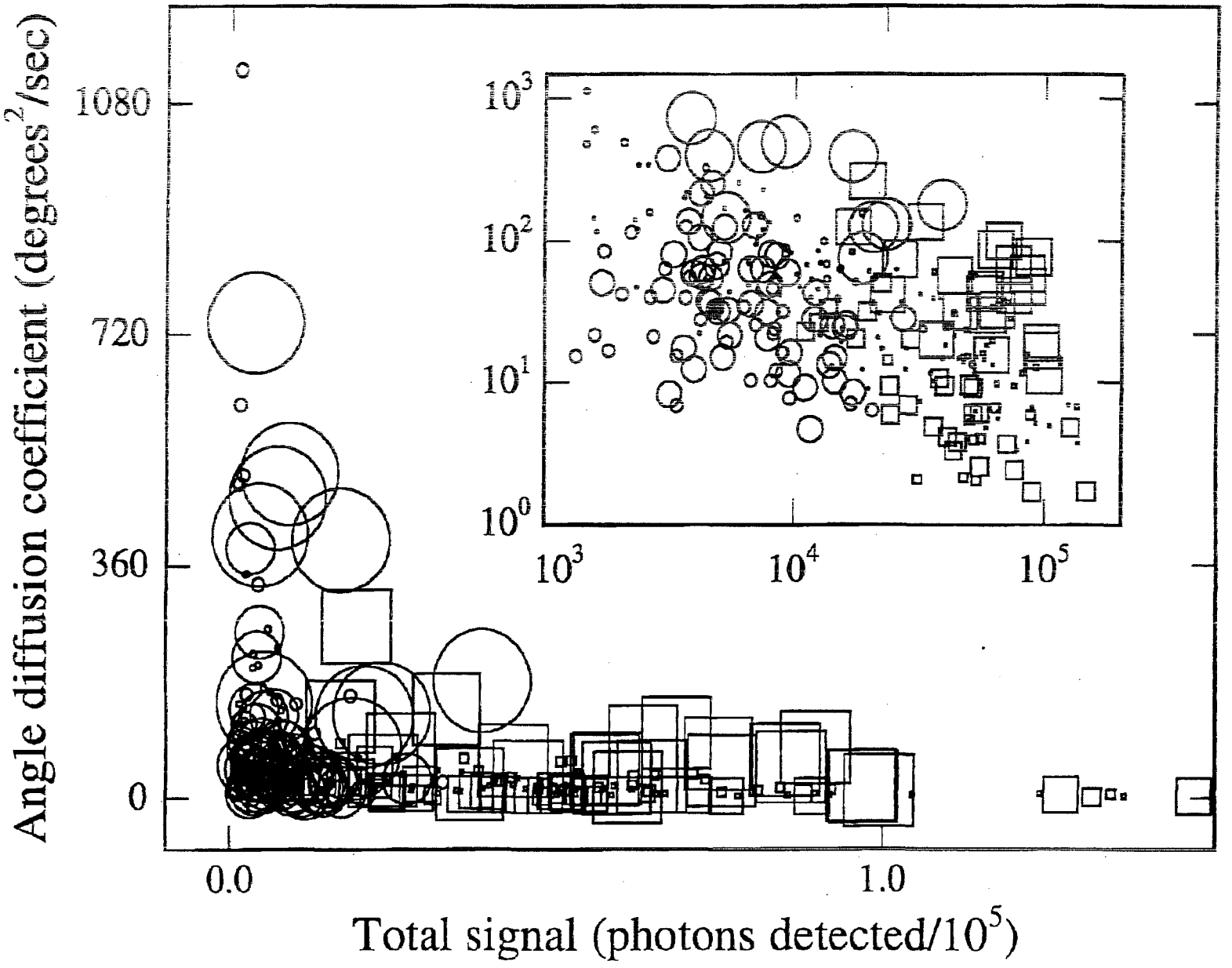
Angle diffusion coefficient (degrees^2/sec)
1080
720
360
0
0.0
1.0
Total signal (photons detected/10^5)
10^3
10^2
10^1
10^0
10^3
10^4
10^5

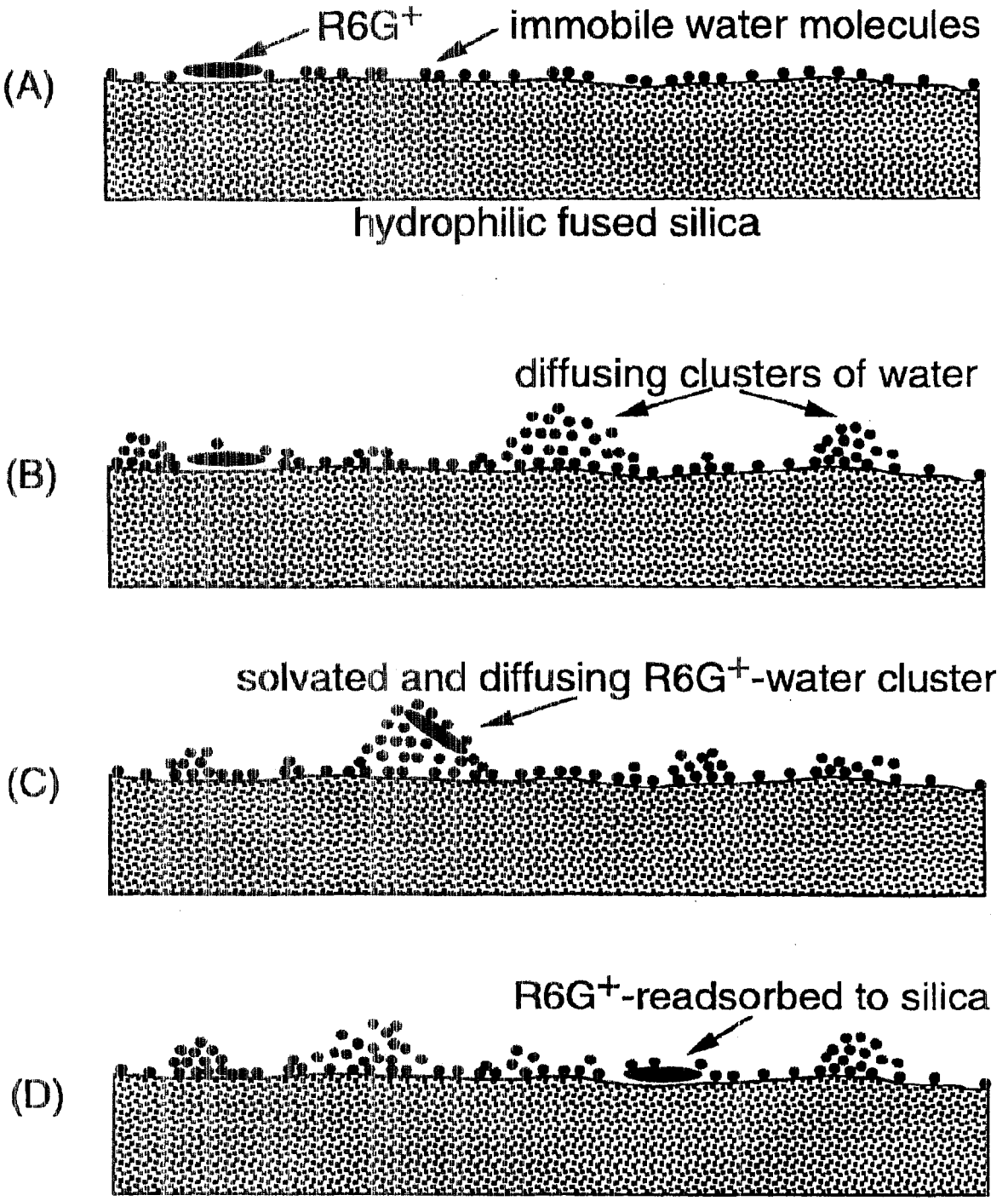
R6G+
immobile water molecules
(A)
hydrophilic fused silica
diffusing clusters of water
(B)
solvated and diffusing R6G+-water cluster
(C)
R6G+-readsorbed to silica
(D)

Fig. 1